Biodegradable active food packaging structures based on hybrid cross-linked electrospun polyvinyl alcohol fibers containing essential oils and their application in the preservation of chicken breast fillets.

Gülden Göksen[1,2], Maria José Fabra[1,3], A. Pérez-Cataluña[1], H. Ibrahim Ekiz[2], Gloria Sanchez[1], Amparo López-Rubio[1,3*]

[1] Department of Preservation and Food Safety Technologies, IATA-CSIC, Av. Agustín Escardino 7, 46980 Paterna, Valencia, Spain.

[2] Department of Food Engineering, Mersin University, Ciftlikkoy, Mersin 33343, Turkey

[3] Interdisciplinary Platform for Sustainable Plastics towards a Circular Economy- Spanish National Research Council (SusPlast-CSIC), Madrid, Spain

*Corresponding author: Tel.: +34 963900022; fax: +34 963636301

E-mail address: amparo.lopez@iata.csic.es (A. López-Rubio)

ABSTRACT

Active food packaging materials produced through electrospinning of polyvinyl alcohol (PVOH) containing essential oils (EOs) from two broadly used spices (*Laurus nobilis* – LEO- and *Rosmarinus officinalis* -REO-) were developed and applied to chicken breast fillets with the aim of prolonging their shelf-life. Citric acid (CA) was successfully incorporated as a natural cross-linker and the developed electrospun structures were heat-treated to promote both the crosslinking and the crystallization of the PVOH matrix. Initially, the morphology, water solubility, physicochemical and thermal properties of the developed structures were evaluated. Then, the antioxidant and antibacterial efficiency of PVOH-EOs hybrid structures were evaluated when directly applied onto an inoculated side of chicken breast fillets. These annealed active food packaging structures containing EO and CA exhibited improved water resistant and thermal stability with respect to their non-crosslinked counterparts. Although part of the EOs content was degraded after the annealing process, the remaining amount in the PVOH samples inhibited the lipid oxidation process up to 68% and displayed enhanced antimicrobial effectiveness when applied onto chicken breast fillets, having a beneficial effect on both the pH and color parameters during storage.

Keywords

Active packaging; electrospinning; biodegradable materials; food coatings

1. INTRODUCTION

Biodegradable packaging materials have recently gained attention in the food industry due to consumer´s awareness of associated environmental benefits. Among them, polyvinyl-alcohol (PVOH) is a water soluble petroleum-based polymer with very good optical properties, non-toxicity, biocompatibility, biodegradability and good film-forming ability to be used as food packaging (Aslam, Kalyar, & Raza, 2018; Shi et al., 2008; Tian, Yan, Rajulu, Xiang, & Luo, 2017). These intrinsic characteristics make PVOH an interesting material for the development of active packages or coatings of great interest in the food area. The development of active materials aiming at maintaining or enhancing the quality and safety of packaged food through the incorporation of antimicrobial and/or antioxidant natural compounds is, in fact, an active research area (Chen et al., 2018; Fang, Zhao, Warner, & Johnson, 2017; Kwon, Chang, & Han, 2017; Neo et al., 2013). However, the most widely used processing methods for the development of packaging materials require high temperatures which could compromise the active properties of many of antimicrobials and antioxidant compounds, as most of them are thermosensitive (i.e. essential oils) (Atarés & Chiralt, 2016; M. Ramos, Jiménez, Peltzer, & Garrigós, 2012).

To counteract this problem, electrospinning has been lately proposed as an alternative to develop active food packaging materials (Estevez-Areco, Guz, Candal, & Goyanes, 2018; Fabra, Lopez-Rubio, & Lagaron, 2016; Lin, Mao, Sun, Rajivgandhi, & Cui, 2019; Pinheiro Bruni et al., 2020). By means of this technique, encapsulation structures can be developed by applying electrostatic forces between a solution of the biopolymer and a grounded collector without the need of using high temperatures for drying the materials, as the solvent is evaporated during the flight of the solution towards the collector due to

the whipping of the biopolymer caused by the high voltage application (Anu Bhushani & Anandharamakrishnan, 2014; Zhang et al., 2019). Therefore, this technology provides several advantages in preserving the functionality of the active compound encapsulated within the electrospun fibers.

As active compounds, essentials oils (EOs) have attracted extensive research, because apart from being a natural product, they have also demonstrated numerous biological activities like, for instance, antimicrobial, antioxidant or anti-inflammatory amongst others (Brahmi et al., 2016; Gómez-Estaca, López de Lacey, López-Caballero, Gómez-Guillén, & Montero, 2010; Yen, Hsieh, Hsieh, Chang, & Wang, 2015). Specifically, essential oils from bay (*Laurus nobilis*) and rosemary (*Rosmarinus officinalis*) have received much attention because of their antimicrobial and antioxidant properties (Göksen, Fabra, Ekiz, & López-Rubio, 2020; Ojeda-sana, Baren, Elechosa, Juárez, & Moreno, 2013; C. Ramos et al., 2012).

However, one of the drawbacks of PVOH as a matrix to include the essential oils is its high water solubility which limits its application in real foods with high water activities. To overcome this problem, several strategies have been carried out in the literature, including mixtures with other polymers (Çay, Miraftab, & Perrin Akçakoca Kumbasar, 2014; Peresin et al., 2014; Yang, Li, & Nie, 2007) and the use of cross-linking agents (Shi et al., 2008) in order to improve the functionality and applicability of PVOH-based materials. Crosslinking can be achieved applying either physical (heat treatment, gamma irradiation, ultraviolet) or chemical agents (glutaraldehyde, formaldehyde) (Mansur, Sadahira, Souza, & Mansur, 2008; Miraftab, Saifullah, & Çay, 2015). However, most of these treatments have been reported to be harmful. For instance, migration of metal ions, used as cross-linkers, could exert cytotoxic effects (Lee & Mooney, 2001). Other crosslinking chemical agents such as glutaraldehyde are highly toxic and are prone to

leach out from the packaging material to the food, thus compromising food safety (Lin, Gu, & Cui, 2018). As an alternative, citric acid (CA), a food-grade compound (Suganthi et al., 2018), has been proposed in this work as a crosslinking agent to keep the integrity of the PVOH materials once in contact with high water activity food products (Stone, Gosavi, Athauda, & Ozer, 2013).

This proof-of-concept study proposes a new route for the development of novel active packaging structures of interest in food preservation. Therefore, based on the considerations outlined above and potential applications of active films, the objectives of the present work were to develop PVOH active films by means of electrospinning and to investigate the influence of the crosslinking treatment on the morphology, thermal and physicochemical properties of the developed structures. Finally, their application as a potential antimicrobial and antioxidant food packaging material has been evaluated in chicken breast fillets.

2. MATERIALS AND METHODS

2.1. Materials

Laurus nobilis essential oil (LEO) and *Rosmarinus officinalis* essential oil (REO) were obtained according to Göksen et al., (2020). Specifically, the composition of REO and LEO was previously determined (Göksen et al., 2020), and the main compound found in both essential oils was 1,8 cineole (55.80 % and 69.87%, respectively).

Polyvinyl alcohol (PVOH) was purchased from Plásticos Hidrosolubles S.L. (Valencia, Spain) and citric acid (CA) was obtained from Sigma-Aldrich (St. Louis, Mo., U.S.A). The strain of *Listeria monocytogenes* CECT 4032 (NCTC 11994) was obtained from the Spanish Type Culture Collection (CECT, Valencia, Spain). Oxford-Listeria-selective agar base was purchased from Thermo Scientific-Oxoid (Basingstoke, UK). Fresh

chicken breast slices were purchased from a local supermarket in Valencia (Spain) and immediately transported to the laboratory and kept under refrigerated conditions.

2.2. Preparation of electrospinning solutions

PVOH solutions were prepared by dissolving 14 g PVOH powder in 100 mL distilled water at 60 °C under magnetic stirring at 300 rpm. Aqueous solutions containing CA were similarly prepared and then, 5 g of CA were incorporated into the PVOH solution under stirring for another 2 h. Aqueous solutions containing LEO or REO essential oils (EOs) were prepared by adding 10 g of each EOs into the as-prepared PVOH aqueous solution and stirred for 2 h to obtain homogeneous solutions. Compositions and nomenclature of each formulation are compiled in Table 1.

Table 1. Composition and properties of electrospinning solutions.

Sample code	%PVA(w/v)	%Citric acid (w/w)	%LEO (w/w)	%REO (w/w)
PVA	14	0	0	0
PVAc	14	5	0	0
PVA/LEO	14	0	10	0
PVAcLEO	14	5	10	0
PVA/REO	14	0	0	10
PVAcREO	14	5	0	10

PVA: Polyvinyl alcohol; c: citric acid; LEO: *Laurus nobilis* essential oil; REO: *Rosmarinus officinalis* essential oil

2.3. Characterization of electrospinning solutions

The Wilhemy plate method was used to measure the surface tension of the biopolymer solutions using the in EasyDyne K20 tensiometer (Krüss GmbH, Hamburg, Germany). The viscosity of the electrospinning solutions was measured using a rotational viscosity meter (Visco Basic Plus L) from Fungilab S.A. (San Feliu de Llobregat, Spain) using spindle no TL1 at 12 rpm. The electrical conductivity and pH of the solutions were determined using a conductivity meter (XSCon6) and pH meter (XS pH50) from Labbox (Barcelona, Spain). All measurements were done in triplicate at 25 ± 2 °C.

2.4. Electrospinning process and post-treatment of the fibers

The electrospinning solutions were loaded into 5 mL plastic syringes connected to an 18-gauge stainless steel nozzle with horizontal configuration. This process was carried out by an electrospinning apparatus including high-voltage (0–30 kV) power supply (Acopian, USA), a syringe pump (KD Scientific, USA) and a collector plate. The flow rate of the solutions, applied voltage and tip-to-collector distance were set to 0.15–0.20 mL/h, 18 kV and 10 cm, respectively, based on preliminary optimization trials. The electrospinning process was carried out under ambient conditions (20 ºC and 58% RH). After the electrospinning process, the samples were cured in an oven at 170 °C for 10 min to foster materials' crosslinking with/without CA. The temperature and time were fixed based on screening experiments.

2.5. Scanning electron microscopy (SEM)

The morphology of the nanofibers was analyzed using a scanning electron microscope (SEM) (Hitachi S-4800, Matsuda, Japan) at an accelerating voltage of 10 kV and working

distance of 8-16 mm. The samples were coated with gold-palladium sputtering under vacuum (Pinheiro Bruni et al., 2020). After analysis, the diameters of the fibers from SEM micrographs were measured using ImageJ software (Image J, NIH, Maryland, USA).

2.6. Fourier transform infrared spectroscopy (FT-IR) analysis

Electrospun fiber mats were characterized using FT-IR spectrometer (Bruker Rheinstetten, Germany). The scans were recorded in the spectral range from 650 to 4000 cm^{-1}. All spectra were collected with a resolution of 4 cm^{-1} by averaging 16 scans.

2.7. Thermal properties of electrospun fibres

Thermal properties of the electrospun mats were characterized using differential scanning calorimetry (DSC) (Perkin Elmer, Inc., DSC 7) and thermogravimetric analysis (TGA) (TA Instruments model Q500 TGA). For TGA, the samples (approximately 10 mg) were heated up from 25 °C to 600 °C at a heating rate of 10 °C min^{-1} under dynamic nitrogen atmosphere. TGA curves express the weight of the sample as a function of temperature. For DSC analysis, samples (between 2-5 mg) were heated of 10 °C min^{-1} from 20 to 290 °C under nitrogen gas and using an empty pan as a reference. Indium was used for calibration and the thermograms from an empty pan were used for correcting the slope of the thermal scans from the samples. All tests were carried out, at least, in duplicate.

The degree of PVOH crystallinity was calculated from the ratio:

$$\chi_c\,(\%) = (\Delta H_m/\Delta H_m^0) \times 100 \qquad \text{(Equation 1)}$$

where $\Delta H_m^0 = 138.6$ J g^{-1} is the melting enthalpy for a perfect 100% PVOH crystal (Jiang, Qiao, & Sun, 2006).

193 **2.8. Challenge tests**

194 Fresh chicken breast fillets (0.80 g carbohydrate, 22.18 g protein, 1.54 g fat content per
195 100 g) were purchased from a local market in Valencia (Spain) and transferred to the
196 laboratory within 1 h and kept under refrigerated conditions. These fillets were aseptically
197 cut into pieces of 10 g and covered with the electrospun structures. The prepared samples
198 were then placed in sterile petri dishes and petri dishes were sealed with parafilm and
199 stored at 4 °C up to 7 days. The physicochemical and microbiological analyses were
200 performed, in triplicate, at 0, 1, 4 and 7 days of storage. The antioxidant analysis was
201 carried out, in triplicate, at the beginning and at the end of the storage time. Four different
202 groups were prepared: uncovered fillets (control) and fillets covered (directly contacting
203 the pieces of chicken) with the cross-linked fibers (PVOHc, PVOHcLEO, PVOHcREO).
204 The pH and color parameters of the samples were measured at each storage time. Briefly,
205 chicken breast samples (10.0 g) were homogenized with 90 mL of distilled water for 1
206 min using a homogenizer (MICCRA GmbH, Heitersheim, Germany). Then, the
207 homogenate was used for determination of pH value (Gonzales-Fandos, Herrera, & Maya,
208 2009). Color parameters (CIE L*, a* and b*) of chicken breast samples were determined
209 using Chroma Meter-CR 400 (Konica Minolta Japan).
210 The lipid oxidation was evaluated by means of the thiobarbituric acid reactive substance
211 (TBARS). The TBARS value was evaluated with the 2-thiobarbituric acid (TBA)
212 distillation method described by Fontes-Candia, Erboz, Martínez-Abad, López-Rubio, &
213 Martínez-Sanz, (2019) with a slight modification. Briefly, 10.0 g of chicken breast meat
214 were homogenized with 30 mL of water. The homogenate was transferred to a distillation
215 flask (500 mL) with 65 mL of water and then the pH was adjusted to 1.5 with using HCl
216 (4N). Ethanolic propyl gallate (10%, 1 mL), EDTA (10%, 1 mL), and a drop of anti-
217 foaming agent were added to mixture. The flask was connected to a Soxhlet apparatus

and the mixture was boiled until 50 mL of distillate were gathered. After distillation, 5 mL of TBA reagent (0.02M TBA in 90% acetic acid) were added to 5 mL of the distillate and placed in a boiling water bath for 40 min of reaction. As a control, 5 mL of distilled water were used instead of the distillate. After cooling at room temperature, the absorbance was measured at 535 nm in a spectrophotometer (Santa Clara, CA, USA). TBARS value was calculated by multiplying the absorbance readings by a factor of 7.8 and expressed as mg malondialdehyde (MDA)/kg meat. The inhibition of lipid oxidation was determined after 7 days as follows:

$$Inhibition\ (\%) = \frac{(TBARS_{blank} - TBARS_{electrospun})}{(TBARS_{blank} - TBARS_{day\ 0})} \times 100 \qquad \text{(Equation 2)}$$

In this equation, $TBARS_{day\ 0}$ corresponds to the TBARS in the uncovered fresh chicken breast meat at day 0 and $TBARS_{blank}$ and $TBARS_{day\ 7}$ refer to the TBARS in the control sample (uncovered fresh chicken breast) and in the different meat samples covered with the electrospun materials after 7 days of refrigerated storage, respectively.

The antimicrobial assays were carried out as follows: chicken breast fillets (10 g) were sterilized by immersion in ethanol 70% for 5 min. Before packing, the samples were soaked in the bacteria suspension of *L. monocytogenes* (approximately 10^8 CFU/mL) and left under a laminar flow safety cabinet for 15 min for attaching inoculums onto chicken breast meat surface. Later on, the samples were packaged individually with the nanofibers (5x5 cm) previously sterilized with UV light for 30 min. Packaged and control samples (unpackaged) were placed into sterile petri dishes and sealed with parafilm and then stored at 4 °C. *L. monocytogenes* presence in the different samples was evaluated by plate counting at different time intervals (0, 1, 4 and 7 days) during cold storage.

2.9. Statistical Analysis

All results were presented as the average ± standard deviation. Statistical analysis was performed by analysis of variance (ANOVA) with SPSS software (version 17.0; IBM Corp., Armonk, NY) using Tukey's test.

3. RESULTS AND DISCUSSION

3.1. Development and characterization of active fibers containing LEO or REO.

Initially, the physicochemical properties of the electrospinning solution were evaluated and correlated with the morphology of developed fibers. Different sizes and morphologies can be obtained through electrospinning processing of biopolymer solutions depending on solution properties (surface tension, viscosity, electrical conductivity) and process parameters. In this work, CA was added as a PVOH crosslinking agent (in combination with an annealing process required for effective crosslinking) in order to avoid the disintegration of electrospun fibers once they would be in direct contact with food, since most of them present high water activity.

PVOH-based solutions with and without CA or EOs were initially characterized and the results are compiled in Table 1S of the Supplementary Material. pH values of the PVOH solutions were around 5.3 at room temperature and they significantly decreased ($p < 0.05$) with the incorporation of CA due to its acidic nature. The addition of CA resulted in a slight increase in the viscosity values of the biopolymer solution, in agreement to that previously reported by Esparza, Ullah, Boluk, & Wu, (2017), although it did not significantly affect the average diameters of the fibers obtained. In general, the incorporation of EOs made the fluid solutions more viscous (greater apparent viscosity values) than the neat PVOH and PVOHc solutions (see Table 1S) which, surprisingly, resulted in thinner fibers (see Table 2S in the Supplementary Material) thus suggesting

267 that, in this case, the diameter of the fibers was mainly governed by the electrical
268 conductivity of the electrospinning solutions.
269 Concerning the conductivity values, the addition of CA solution provoked a sharp
270 increase ($p<0.05$) in electrical conductivity of the PVOH solution (1081 μS/cm), probably
271 ascribed to the ionic nature of this carboxylic acid in solution. A similar trend was
272 observed in PVOH-EOs solutions containing CA, favoring the formation of slightly
273 thinner fibers during electrospinning as the greater conductivity facilitates jet stretching,
274 as inferred from Table 2S and Figure 1.
275 Regarding the surface tension values, PVOH-aqueous solutions showed surface tension
276 values significantly lower than those of the solvent (72 mN/m). Likewise, the
277 incorporated EOs behaved as surfactants, further decreasing the surface tension values of
278 the solutions. A slight increase in surface tension was observed upon CA addition when
279 compared with their counterparts prepared without the natural crosslinking agent. As
280 deduced from the solution properties, surface tension did not play a major role on the
281 morphology of the fibers which were mainly governed by the increase in the electrical
282 conductivity of the CA-containing solutions, favoring the formation of thinner fibers.
283 The SEM images of PVOH-based fibers (with and without CA and EOs) are displayed in
284 Figure 1. Table 2S of the Supplementary Material gathers the average diameter of the
285 electrospun fibers before and after the annealing process used to promote the PVOH-CA
286 crosslinking. The size measurements from the SEM micrographs revealed that the
287 average diameter of fibers decreased with the incorporation of both essential oils
288 (LEO/REO) and CA, mainly ascribed to the increase in electrical conductivity.
289 Interestingly, a significant increase ($p<0.05$) in the average diameter was clearly observed
290 in PVOH and PVOH/EOs films after the annealing process. In contrast, this increase was
291 significantly lower if the electrospun coatings had CA, suggesting that interactions

between the PVOH and CA preserved the morphology and porous structure of the coating, and thus the integrity of the fibers, to a greater extent. The increase in the average diameter of the electrospun fibers in annealed films prepared without CA can be attributed to a partial melting of the PVOH matrix and subsequent aggregation of the PVOH-based fibers during the heat treatment, as it is clearly observed in the images B, E and H of Fig. 1A.

As most food products present high water activity, the integrity of the PVOH-based electrospun fibers upon water immersion was also evaluated and their morphology after immersion and subsequent drying was analyzed by SEM in order to evaluate the effect of crosslinking on water resistance. As expected, when CA was not used, the fibrillar morphology of the electrospun PVOH/EOs films was completely lost after water immersion (Images C, F and I of Fig. 1A), as previously reported by other authors (Çay & Miraftab, 2013; Destaye, Lin, & Lee, 2013). In contrast, the cross-linked films kept their fibrillary morphology (although a certain swelling was observed as deduced from the increase in the average fiber diameter- see Table 2), providing a better stability and evidencing the efficacy of the annealing process in promoting the esterification reaction between carbonyl groups in CA and hydroxyl groups in PVOH (see Figure 1B). In general, crosslinking reduces the interstitial spaces between the biopolymer chains, thus reducing molecular motion and preventing extensive swelling of the electrospun fibers (Çay & Miraftab, 2013; Miraftab et al., 2015; Santiago-Morales, Amariei, Letón, & Rosal, 2016).

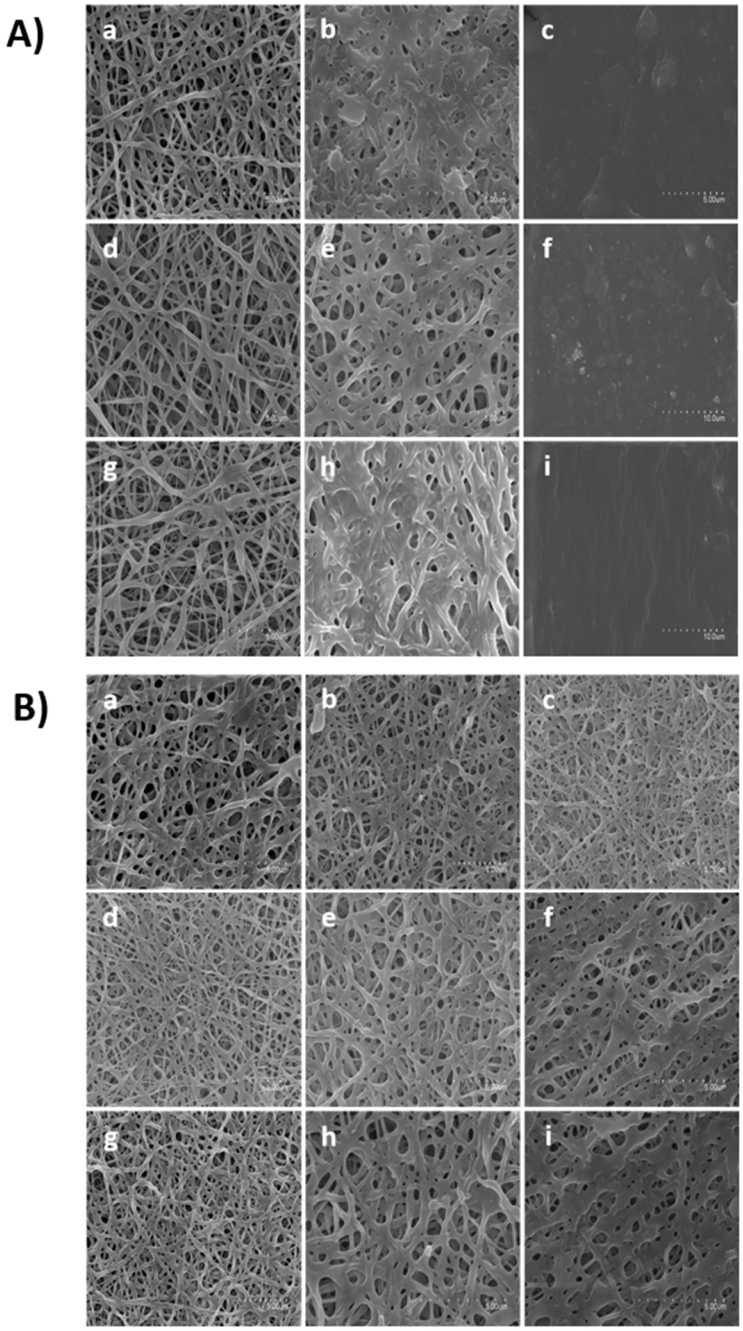

Figure 1. SEM images of: **A)** PVOH, PVOH/LEO and PVOH/REO nanofibers and **B)** PVOHc, PVOHcLEO and PVOHcREO nanofibers, before annealing (a, d, g), after annealing (b, e, h) and after water immersion (c, f, i).

Infrared spectroscopy was used to evaluate the changes in the molecular structure of the different electrospun mats obtained. As very similar spectra were obtained for the mats

with the two different EOs, only the ones containing LEO are shown for clarity. ATR-FTIR spectra of the neat and LEO-loaded PVOH or PVOH/CA electrospun films before and after the annealing process are gathered in Figure 2. The spectrum of neat PVOH, as previously described, showed an intense band between 3600 and 3200 cm^{-1} ascribed to the stretching of O-H groups and other characteristic bands between 2840 and 3000 cm^{-1}, attributed to the stretching C-H from alkyl groups and between 1757-1710 cm^{-1} corresponding to the C=O stretching and C-O from acetate groups remaining from PVOH (Andrade, Barbosa-Stancioli, Mansur, Vasconcelos, & Mansur, 2008; Mansur et al., 2008).

For comparison purposes, the different spectra were normalized to the vibrational band at 1232 cm^{-1}, assigned to the stretching vibration of C-O arising from alcohol and ester groups (Esparza et al., 2017). Upon EOs incorporation, no significant shifts were observed in the spectral bands of the neat PVOH or PVOH/CA independently of the final compositions of the films, thus, suggesting that EOs were not chemically interacting with the PVOH network. However, a decrease in the OH stretching band was seen upon EO incorporation.

Annealing is known to promote crystal formation in polymeric materials. From Figure 2A, it can be clearly seen that annealing caused an increase in the OH stretching band centered at 3300 cm^{-1}, probably indicating stronger hydrogen bonding interactions. Another remarkable change, was the intensity increase in the range from 1000-1100 cm^{-1} (C–O stretching in C–O–H groups and C-O-C groups), thus probably indicating that this area could arise from crystallizable chain segments in PVOH.

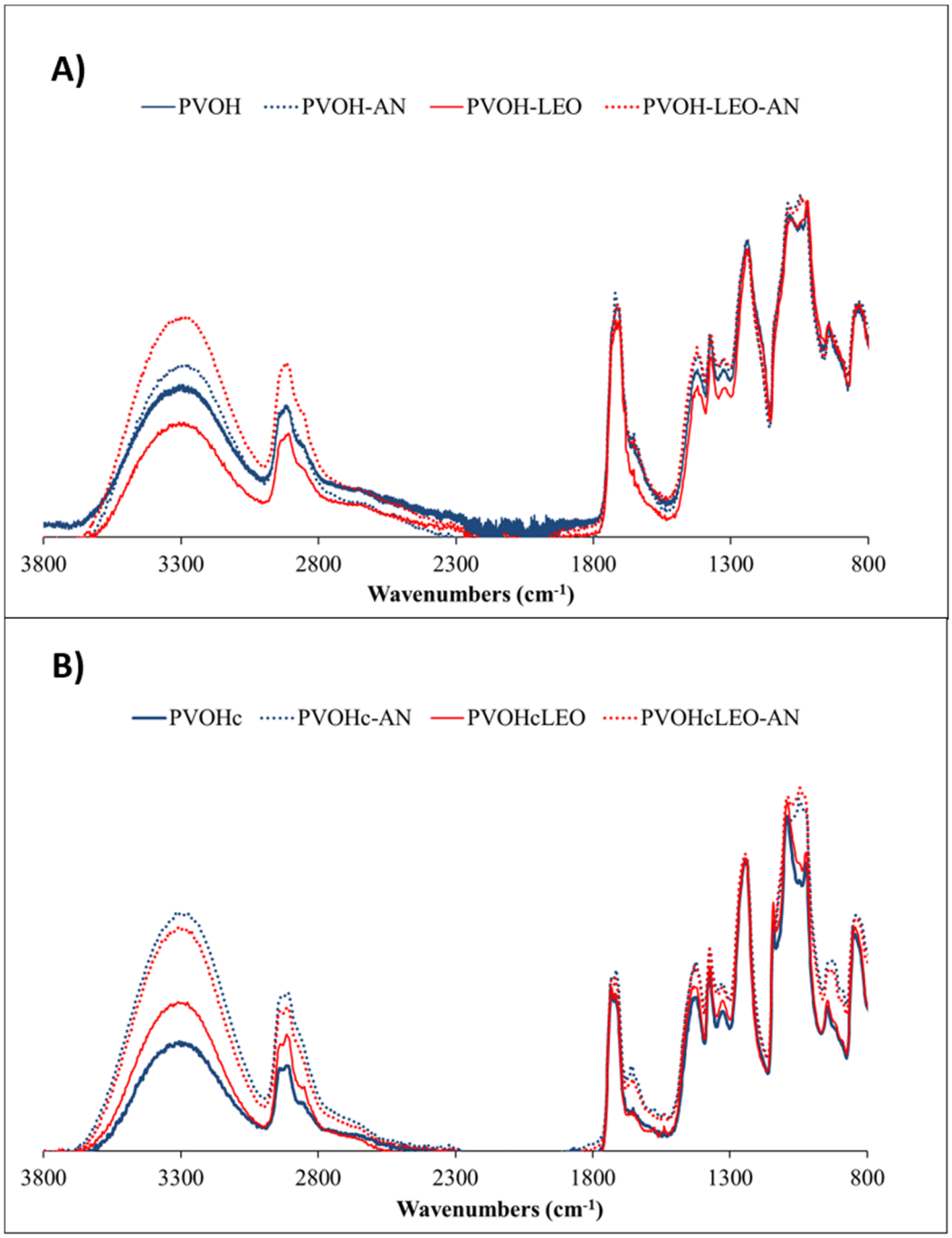

Figure 2. ATR-FTIR of: **A)** neat and LEO-loaded PVOH electrospun fibers and **B)** neat and LEO-loaded PVOH/CA electrospun fibers before and after the annealing process (indicated by -AN).

In contrast, additional spectral changes were observed in the samples containing CA (Figure 2B). Similar to what was observed in the mats without CA, the heat treatment

caused an increase in the OH stretching band and in the range from 1000-1100 cm^{-1}, both probably indicating increased molecular order in the PVOH chains. But apart from these changes, an increase in the bands from 1700 to 1750 cm^{-1} arising from ester and carboxylic bonds was also observed in the heat-treated samples, thus confirming the crosslinking reaction. Presumably, during the heat treatment process, CA is first dehydrated to its anhydride and subsequently, the ester group is formed through the ring opening of the citric acid anhydride by the –OH groups present in the PVOH backbone and this process is repeated to complete the crosslinking (Nikfarjam, Taheri Qazvini, & Deng, 2014).

The thermal stability of the electrospun fibres was also assessed by thermogravimetric analysis. As very similar thermograms were obtained for the mats with the two different EOs, only the ones containing LEO are shown for clarity. Figure 3 shows the thermogravimetric curves of the neat and LEO-loaded PVOH or PVOH/CA electrospun films before and after the annealing process. Neat PVOH showed a first stage of mass loss (25 - 150 ºC), attributed to the loss of water molecules (both weakly and strongly interacting with the polymer). The second phase of mass loss (200 - 375 ºC) has been associated to the decomposition of the side chains of PVOH and the third stage ranging from 375 to 500 ºC has been mainly related with polymer main chain degradation (Van Etten et al., 2014). Thus, the last two stages were responsible for the mass loss of around 92%, which corresponded to the structural decomposition of PVOH.

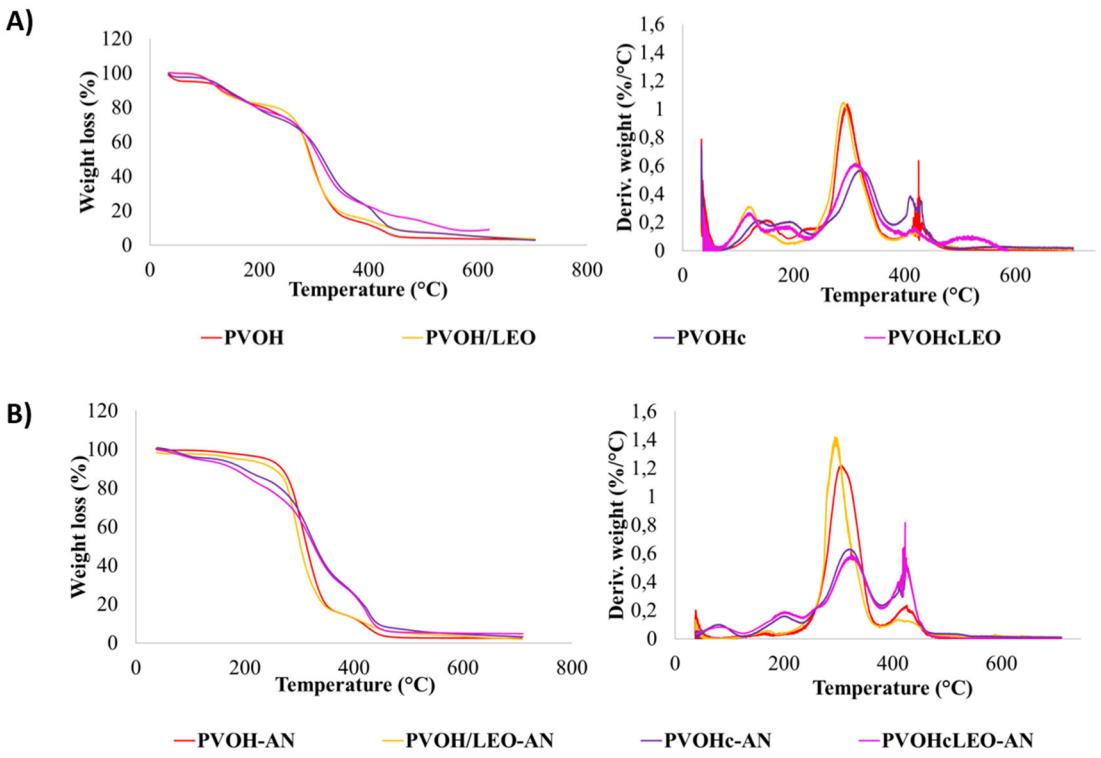

372

373 **Figure 3.** TG and DTG curves of **A)** neat and LEO-loaded PVOH and PVOH/CA
374 electrospun fibers **A)** before and **B)** after the annealing process (indicated by -AN).

375

376 Considering that the neat LEO and REO had only one degradation peak (~ 88ºC)
377 corresponding to the evaporation of the volatile compounds present in the essential oils
378 (Göksen et al., 2020), the shift to higher temperature (~ 120 ºC) observed when the EOs
379 were incorporated within the PVOH matrices, suggest that the polymer increased their
380 thermal stability.

381 Interestingly, a new degradation peak at around ~ 185 ºC (see Figure 3) appeared in the
382 samples containing CA, which probably corresponds to the degradation temperature of
383 neat CA, as it has been previously reported to occur in a single-step between 160 and 220
384 ºC (Wyrzykowski, Hebanowska, Nowak-Wiczk, Makowski, & Chmurzyński, 2011).

385 After the annealing process, a smoother peak was found at higher temperature (~ 162 ºC)
386 in PVOH-LEO-AN, evidencing that EOs were mostly degraded due to the annealing

387 treatment carried out at 170 ºC, at a much higher temperature than the degradation
388 temperature of both LEO and REO. It was also observed that the main degradation peak
389 of PVOH was shifted to lower temperatures in PVOH-EOs-AN samples, indicating that
390 the presence of LEO or REO detrimentally affected the degradation temperature of neat
391 PVOH. Interestingly, a new degradation peak centered at ~ 89 ºC was found in annealed
392 samples containing CA, even in those prepared without EOs, suggesting the presence of
393 less heat-stable molecules which were probably formed during the annealing, which
394 degraded at this temperature.
395 Furthermore, one of the main changes that occurred after the annealing process was
396 related to the stability of the PVOH macromolecules cross-linked with the CA. In fact,
397 the thermal degradation during the second and third weight loss stage occurred more
398 gradually and started at higher temperatures when CA was present, thus suggesting that
399 the interactions between CA and PVOH had a protective impact on the thermal stability
400 of the developed electrospun fibers. Thus, TGA results suggest that crosslinking had a
401 positive effect on the thermal stability of the polymer material, while the inclusion of the
402 essential oils had the opposite effect.
403 The degree of crystallinity has important effects in the physical properties of biopolymers.
404 Thus, the thermal properties of the PVOH and PVOH/CA films and the active films
405 containing EOs were also investigated by DSC analysis. Table 2 compiles the temperature
406 of melting (T_m), as well as the melting enthalpy (ΔH_m) and crystallinity (X_c) obtained
407 from the first heating run. ΔH can be used to estimate the crystallinity of a polymer
408 sample.
409 Interestingly, just after electrospinning, i.e. without an annealing process, the fibers
410 obtained were amorphous and no thermal transition was seen through DSC. In contrast,
411 the annealing process promoted crystal development, which was different depending on

412 the initial composition of the fibers. As seen in Table 2, the presence of EOs, increased
413 the melting point of the annealed fibers, indicating that the crystals present in the materials
414 were bigger or more perfect. This could be ascribed to a plasticization effect of the oils,
415 facilitating chain mobility and packing during the annealing process, fact which led to
416 higher melting temperature and higher melting enthalpy. In contrast, Lan et al., (2019)
417 stated that the addition of d-limonene in PVOH matrices hindered crystallization of the
418 PVOH molecules, thus resulting in lower melting temperature and enthalpy which was
419 ascribed to the d-limonene impeding hydrogen bonding not only within PVOH molecules
420 but also between PVOH molecular chains. Similarly, Hernández-López et al., (2019)
421 reported an ΔH decrease when pine essential oil was added to PLA-based composite
422 fibers, indicating that the incorporation of the dispersed phase into the matrix reduced the
423 crystallization of the biopolymer matrix. It should be stressed, however, that in the
424 thermal data provided in the mentioned works was obtained after erasing the thermal
425 history of the materials, while in our case the thermal parameters were obtained during
426 the first heating ramp. Regarding the effect of citric acid incorporation, similarly no
427 transition was observed before annealing, while after this heat treatment crosslinking was
428 promoted, thus limiting the ability of polymeric chains to reorganize, thus, resulting in
429 lower melting points, although similar crystallinity values. This implies that although the
430 amount of crystals formed during annealing was similar in the samples with or without
431 citric acid, they were smaller or less perfect when crosslinking took place.
432
433 **Table 2.** Parameters from DSC curves of annealed electrospun fibers.

Sample	**Peak Temp. (°C)**	**Melting Enthalpy (J/g)**	**Onset Temp. (°C)**	**End Temp. (°C)**	**Xc (%)**
PVA	178.4±1.1[a]	16.1±1.4[a]	160.2±1.8[a]	191.0±1.0[a]	11.6±1.0[a]

PVA/LEO	189.7±6.5^{b}	26.6±10.2^{a}	158.4±5.1^{a}	205.8±1.0^{b}	19.2±7.4^{a}
PVA/REO	194.6±0.4^{b}	24.2±11.1^{a}	173.4±1.3^{b}	207.9±8.7^{b}	17.4±8.0^{a}
PVAc	166.1±0.7^{c}	16.8±2.3^{a}	145.5±4.4^{c}	181.2±3.4^{c}	12.6±1.6^{a}
PVAcLEO	184.5±1.0^{b}	29.4±10.3^{a}	155.9±6.8^{ac}	201.4±2.6^{b}	21.2±7.4^{a}
PVAcREO	179.2±2.0^{a}	18.9±5.8^{a}	154.0±1.8^{a}	194.7±2.8^{a}	13.6±4.2^{a}

Mean values ± standard deviations (n=3). Different letters at column denote significant differences ($p<0.05$).

3.2. Challenge tests

Challenge tests on chicken breast fillets were carried out to ascertain the antioxidant and antimicrobial effectiveness of the active fiber mats on real food samples. Although TGA analysis revealed that EOs were mostly degraded during the annealing process, the functional properties of the developed electrospun fibers were tested to determine if the LEO or REO remaining after the annealing process had antioxidant and antimicrobial properties. In fact, previous works carried on EOs loaded-casting films revealed antilisterial activity even though the losses of volatile compounds during the film drying ranged between 39 and 99 %, depending on the EOs and EOs:biopolymer ratio (Sánchez-González, Vargas, González-Martínez, Chiralt, & Cháfer, 2011).

Initially, the physicochemical quality of the packaged and unpackaged samples was evaluated in terms of pH and color parameters. Table 3S from the Supplementary Material shows the changes in the pH values during the storage in the different chicken samples covered by electrospun structures. The initial pH value of the fillet was ~ 5.97. The pH development in the chicken breast fillets can be affected by both the microbial growth and the oxidation process which occurred to a different extent in the different packaged samples. As expected, the pH of unpackaged samples slightly increased during the storage

454 time, ranging between 5.97 and 6.81. This agrees with the fact that foods stored under
455 aerobiosis and rich in proteins and free aminoacids, such as chicken breast fillets, present
456 a pH increase as the number of microorganisms that cause spoilage increases (Křížek,
457 Vácha, Vorlová, Lukášová, & Cupáková, 2004; Ntzimani, Paleologos, Savvaidis, &
458 Kontominas, 2008), as it will be detailed below. Furthermore, the proteolytic activity also
459 results in the production of basic compounds which could contribute to the increase in pH
460 (Vinci & Antonelli, 2002). In contrast, the pH of the packaged samples did not vary
461 significantly during the storage time or it was even slightly decreased, confirming that
462 these samples were better protected.
463 Table 3 shows the changes in the color parameters (L*, a* and b* values) of the food
464 samples during storage at refrigeration conditions (4 °C). L* values decreased during
465 storage in all the samples, indicating that the chicken fillets became darker, change that
466 was more accentuated in unpackaged samples. Regarding the sample redness (a* values),
467 it increased during storage time in unpackaged samples. In contrast, it was significantly
468 lower in packaged chicken breast fillets and there was a trend to decrease during the
469 storage time in those prepared with electrospun fibers containing EOs, suggesting some
470 interaction between the essential oils and the meat pigments, thus affecting redness. The
471 sample yellowness (b* values) increased to a greater extend in unpackaged chicken breast
472 fillets which could be related with the greater lipid oxidation of these samples as it will
473 be detailed bellow.
474
475
476
477

478 **Table 3.** Color measurement of L*, a* and b* values during storage of packaged chicken

479 breast samples

		Storage time (day)			
		0	1	4	7
L*	Control	49.71±1.05^{a1}	49.23±1.05^{a1}	42.75±1.50^{a2}	43.41±0.82^{a2}
	PVOHc	50.08±0.90^{a1}	49.20±1.39^{a1}	47.95±1.05^{b1}	47.15±1.03^{b1}
	PVOHcLEO	55.44±0.79^{b1}	56.09±2.08^{b1}	54.18±0.57^{c1}	51.89±1.35^{c2}
	PVOHcREO	54.60±1.68^{b1}	53.75±1.35^{ab1}	51.54±0.47^{c1}	51.45±0.31^{c1}
a*	Control	2.11±0.05^{a1}	2.37±0.09^{a2}	2.43±0.10^{a23}	2.58±0.06^{a3}
	PVOHc	1.85±0.10^{b1}	2.03±0.11^{b1}	1.91±0.05^{b1}	2.02±0.11^{b1}
	PVOHcLEO	1.87±0.07^{b1}	1.71±0.06^{c2}	0.90±0.06^{c2}	1.12±0.09^{c1}
	PVOHcREO	1.93±0.03^{ab1}	1.88±0.11^{bc1}	0.87±0.08^{c2}	1.04±0.18^{c1}
b*	Control	7.75±0.41^{a1}	8.34±0.33^{a1}	9.36±0.46^{a2}	10.18±0.34^{a2}
	PVOHc	7.69±0.23^{a1}	8.07±0.25^{a1}	8.67±0.22^{a12}	8.84±0.43^{b2}
	PVOHcLEO	7.82±0.12^{a1}	8.56±0.69^{a12}	8.73±0.25^{a2}	8.97±0.18^{b2}
	PVOHcREO	7.54±0.33^{a1}	7.75±0.34^{a1}	8.64±0.30^{a2}	8.75±0.48^{b2}

480 Mean values ± standard deviations (n=3).
481 Different letters in the same column show significant differences ($p<0.05$) among
482 samples.
483 Different numbers in the same file show significant differences ($p<0.05$) during the
484 storage time.
485

Lipid oxidation values during chilled storage of the chicken breast fillets are gathered in Table 4 for the samples covered with the different electrospun structures. Samples packaged with PVOHc structures inhibited lipid oxidation around 19%, whereas samples packaged with EOs-loaded electrospun fibers prevented lipid oxidation to a greater extent, reaching a ~43 and ~65 % of lipid oxidation inhibition for PVOH films prepared with REO and LEO, respectively. The protective effect observed for PVOHc electrospun coatings can be ascribed to the presence of non-cross-linked (free) CA in the chicken samples, which may contribute to improve food quality and shelf-life (Doležalová, Molatová, Buňka, Březina, & Marounek, 2010; Gonzales-Fandos et al., 2009). Interestingly, this effect was enhanced with the incorporation LEO and REO, indicating that even most of the EOs were degraded during the annealing process, the remaining compounds had antioxidant properties as well as antimicrobial activity, as it will be detailed bellow.

Table 4. 2-Thiobarbituric acid reactive substances (TBARS) and estimated lipid oxidation inhibition in fresh chicken breast fillets (day 0) and in the packaged samples after 7 days of storage.

		TBARS (mg MDA/kg)	**Lipid oxidation inhibition (%)**
Day 0	Control	0.29±0.04[a]	-
Day 7	Control	0.91±0.03[b]	0
	PVAc	0.79±0.06[b]	18.71±0.65
	PVAc-LEO	0.51±0.02[c]	64.90±2.35
	PVAc-REO	0.64±0.04[d]	42.95±6.34

Different letters in the same column show significant differences ($p<0.05$).

505 Regarding the antimicrobial activity, viable counts of *L. monocytogenes* after 7 days of
506 incubation at 4 ºC on chicken breasts are displayed in Figure 4. An increase of about 1
507 log in the counts of pathogenic bacteria was observed in the chicken breast controls after
508 7 days of storage. In contrast, samples with PVOHc did not significantly increase the
509 viable counts while a growth inhibition was observed in the chicken breasts packaged
510 with PVOHc/EOs electrospun structures, exhibiting up to 1 log decrease with respect to
511 the initial values and with the PVOH/LEO having slightly more antimicrobial effect than
512 REO.
513 Therefore, in terms of antioxidant and antimicrobial growth, the use of EOs-loaded
514 PVOH films significantly prolonging the shelf life of chicken breast fillets, being LEO
515 more efficient than REO. These differences can be ascribed to the presence of the most
516 active compound, 1,8 cineole, which was present in greater amounts in LEO (~ 69.87 %)
517 than in REO (~55.80 %) (Göksen et al., 2020).

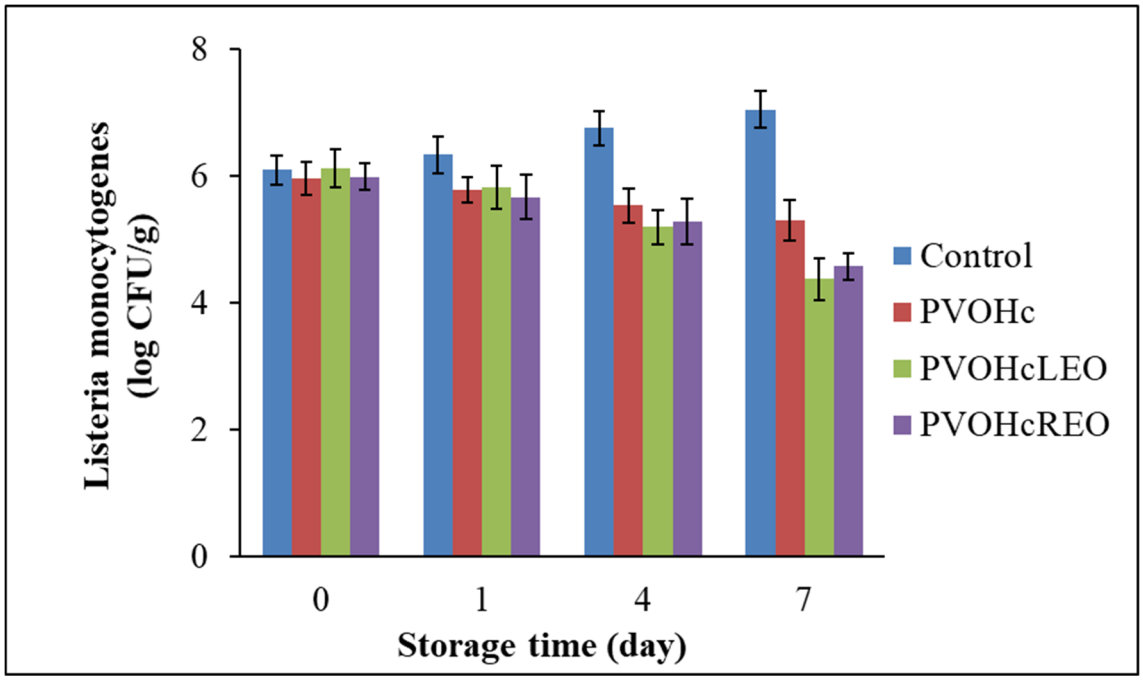

518

519 **Figure 4.** Changes in *L. monocytogenes* (log CFU/g) during the storage of packaged
520 chicken breast samples.

521

4. CONCLUSIONS

Active cross-linked electrospun PVOH fibers were prepared containing two different EOs. Citric acid (CA) was used as a cross-linker together with an annealing process with the aim of maintaining the integrity of the fibers in contact with high moisture foods. The average diameter of the fibers decreased with the incorporation of both EOs and CA, mainly ascribed to the increase in electrical conductivity. The morphology and porous structure of the electrospun fibers containing EOs and PVOH was successfully maintained to a greater extent in annealed samples after being immersed in water, evidencing the efficiency of the crosslinking process. In contrast, this effect was not observed in the annealed electrospun samples prepared without CA.

Furthermore, physicochemical and thermal stability of annealed electrospun PVOH food packaging structures were successfully improved by the incorporation of CA. The materials were tested to improve preservation of chicken breast samples, even though the annealing process probably degraded most of the EOs, as observed through TGA. These active packaging coatings containing LEO and REO enhanced the shelf-life of chicken breast fillets, reducing the lipid oxidation process and reducing *Listeria* counts during cold storage. Therefore, this works provides a simple method to obtain PVOH-coatings with suitable integrity for use in the active preservation of fresh food products like meat.

Acknowledgements

Gulden Goksen thanks to The Scientific and Technical Research Council of Turkey-TUBITAK-BIDEB 2214/A for International Doctoral Research Fellowship Programme (1059B141800428). The authors acknowledge Research Fund of Mersin University in Turkey (Project No: 2017-1-TP3-2274). M.J. Fabra is recipient of a Ramon y Cajal

(RYC-2014-15842) contract from the Spanish Ministry of Economy, Industry and Competitiveness.

REFERENCES

Andrade, G. I., Barbosa-Stancioli, E. F., Mansur, A. A. P., Vasconcelos, W. L., & Mansur, H. S. (2008). Small-angle X-ray scattering and FTIR characterization of nanostructured poly (vinyl alcohol)/silicate hybrids for immunoassay applications. *Journal of Materials Science*, *43*(2), 450–463. https://doi.org/10.1007/s10853-007-1953-7

Anu Bhushani, J., & Anandharamakrishnan, C. (2014). Electrospinning and electrospraying techniques: Potential food based applications. *Trends in Food Science and Technology*, *38*(1), 21–33. https://doi.org/10.1016/j.tifs.2014.03.004

Aslam, M., Kalyar, M. A., & Raza, Z. A. (2018). Polyvinyl alcohol: A review of research status and use of polyvinyl alcohol based nanocomposites. *Polymer Engineering and Science*, *58*(12), 2119–2132. https://doi.org/10.1002/pen.24855

Atarés, L., & Chiralt, A. (2016). Essential oils as additives in biodegradable films and coatings for active food packaging. *Trends in Food Science and Technology*, *48*, 51–62. https://doi.org/10.1016/j.tifs.2015.12.001

Brahmi, F., Abdenour, A., Bruno, M., Silvia, P., Alessandra, P., Danilo, F., … Mohamed, C. (2016). Chemical composition and in vitro antimicrobial, insecticidal and antioxidant activities of the essential oils of Mentha pulegium L. and Mentha rotundifolia (L.) Huds growing in Algeria. *Industrial Crops and Products*, *88*, 96–105. https://doi.org/10.1016/j.indcrop.2016.03.002

Çay, A., & Miraftab, M. (2013). Properties of electrospun poly(vinyl alcohol) hydrogel

nanofibers crosslinked with 1,2,3,4-butanetetracarboxylic acid. *Journal of Applied Polymer Science*, *129*(6), 3140–3149. https://doi.org/10.1002/app.39036

Çay, A., Miraftab, M., & Perrin Akçakoca Kumbasar, E. (2014). Characterization and swelling performance of physically stabilized electrospun poly(vinyl alcohol)/chitosan nanofibres. *European Polymer Journal*, *61*, 253–262. https://doi.org/10.1016/j.eurpolymj.2014.10.017

Çay, A., & Mohsen Miraftab. (2013). Properties of electrospun poly(vinyl alcohol) hydrogel nanofibers crosslinked with 1,2,3,4-butanetetracarboxylic acid. *Journal of Applied Polymer Science*, *129*(6), 3140–3149. https://doi.org/10.1002/app.39036

Chen, C., Xu, Z., Ma, Y., Liu, J., Zhang, Q., Tang, Z., … Xie, J. (2018). Properties, vapour-phase antimicrobial and antioxidant activities of active poly(vinyl alcohol) packaging films incorporated with clove oil. *Food Control*, *88*, 105–112. https://doi.org/10.1016/j.foodcont.2017.12.039

Destaye, A. G., Lin, C. K., & Lee, C. K. (2013). Glutaraldehyde vapor cross-linked nanofibrous PVOH mat with in situ formed silver nanoparticles. *ACS Applied Materials and Interfaces*, *5*(11), 4745–4752. https://doi.org/10.1021/am401730x

Doležalová, M., Molatová, Z., Buňka, F., Březina, P., & Marounek, M. (2010). Effect of organic acids on growth of chilled chicken skin microflora. *Journal of Food Safety*, *30*(2), 353–365. https://doi.org/10.1111/j.1745-4565.2009.00212.x

Esparza, Y., Ullah, A., Boluk, Y., & Wu, J. (2017). Preparation and characterization of thermally crosslinked poly(vinyl alcohol)/feather keratin nanofiber scaffolds. *Materials and Design*, *133*, 1–9. https://doi.org/10.1016/j.matdes.2017.07.052

Estevez-Areco, S., Guz, L., Candal, R., & Goyanes, S. (2018). Release kinetics of rosemary (Rosmarinus officinalis) polyphenols from polyvinyl alcohol (PVOH) electrospun nanofibers in several food simulants. *Food Packaging and Shelf Life*,

596 *18* (August), 42–50. https://doi.org/10.1016/j.fpsl.2018.08.006
597 Fabra, M. J., Lopez-Rubio, A. L., & Lagaron, J. M. (2016). Use of the
598 electrohydrodynamic process to develop active/bioactive bilayer films for food
599 packaging applications. *Food Hydrocolloids*, *55*, 11–18.
600 https://doi.org/10.1016/j.foodhyd.2015.10.026
601 Fang, Z., Zhao, Y., Warner, R. D., & Johnson, S. K. (2017). Active and intelligent
602 packaging in meat industry. *Trends in Food Science and Technology*.
603 https://doi.org/10.1016/j.tifs.2017.01.002
604 Fontes-Candia, C., Erboz, E., Martínez-Abad, A., López-Rubio, A., & Martínez-Sanz,
605 M. (2019). Superabsorbent food packaging bioactive cellulose-based aerogels from
606 Arundo donax waste biomass. *Food Hydrocolloids*, *96*(January), 151–160.
607 https://doi.org/10.1016/j.foodhyd.2019.05.011
608 Göksen, G., Fabra, M. J., Ekiz, H. I., & López-Rubio, A. (2020). Phytochemical-loaded
609 electrospun nanofibers as novel active edible films: Characterization and
610 antibacterial efficiency in cheese slices. *Food Control*, *112*, 107133.
611 https://doi.org/10.1016/j.foodcont.2020.107133
612 Gómez-Estaca, J., López de Lacey, A., López-Caballero, M. E., Gómez-Guillén, M. C.,
613 & Montero, P. (2010). Biodegradable gelatin-chitosan films incorporated with
614 essential oils as antimicrobial agents for fish preservation. *Food Microbiology*,
615 *27*(7), 889–896. https://doi.org/10.1016/j.fm.2010.05.012
616 Gonzales-Fandos, E., Herrera, B., & Maya, N. (2009). Efficacy of citric acid against
617 Listeria monocytogenes attached to poultry skin during refrigerated storage.
618 *International Journal of Food Science & Technology*, *44*, 262–268.
619 https://doi.org/10.1111/j.1365-2621.2007.01673.x
620 Hernández-López, M., Correa-Pacheco, Z. N., Bautista-Baños, S., Zavaleta-Avejar, L.,

621 Benítez-Jiménez, J. J., Sabino-Gutiérrez, M. A., & Ortega-Gudiño, P. (2019). Bio-
622 based composite fibers from pine essential oil and PLA/PBAT polymer blend.
623 Morphological, physicochemical, thermal and mechanical characterization.
624 *Materials Chemistry and Physics*, *234*(October 2018), 345–353.
625 https://doi.org/10.1016/j.matchemphys.2019.01.034
626 Jiang, W., Qiao, X., & Sun, K. (2006). Mechanical and thermal properties of
627 thermoplastic acetylated starch/poly(ethylene-co-vinyl alcohol) blends.
628 *Carbohydrate Polymers*, *65*(2), 139–143.
629 https://doi.org/10.1016/j.carbpol.2005.12.038
630 Křížek, M., Vácha, F., Vorlová, L., Lukášová, J., & Cupáková, Š. (2004). Biogenic
631 amines in vacuum-packed and non-vacuum-packed flesh of carp (Cyprinus carpio)
632 stored at different temperatures. *Food Chemistry*, *88*(2), 185–191.
633 https://doi.org/10.1016/j.foodchem.2003.12.040
634 Kwon, S.-J., Chang, Y., & Han, J. (2017). Oregano essential oil-based natural
635 antimicrobial packaging film to inactivate Salmonella enterica and yeasts/molds in
636 the atmosphere surrounding cherry tomatoes. *Food Microbiology*, *65*, 114–121.
637 https://doi.org/10.1016/J.FM.2017.02.004
638 Lan, W., Liang, X., Lan, W., Ahmed, S., Liu, Y., & Qin, W. (2019). Electrospun
639 polyvinyl alcohol/d-limonene fibers prepared by ultrasonic processing for
640 antibacterial active packaging material. *Molecules*, *24*(4), 767.
641 https://doi.org/10.3390/molecules24040767
642 Lee, K. Y., & Mooney, D. J. (2001). Hydrogels for tissue engineering. *Chemical*
643 *Reviews*, *101*(7), 1869–1879. https://doi.org/10.1021/cr000108x
644 Lin, L., Gu, Y., & Cui, H. (2018). Novel electrospun gelatin-glycerin-ε-Poly-lysine
645 nanofibers for controlling Listeria monocytogenes on beef. *Food Packaging and*

646 *Shelf Life*, *18*, 21–30. https://doi.org/10.1016/J.FPSL.2018.08.004
647 Lin, L., Mao, X., Sun, Y., Rajivgandhi, G., & Cui, H. (2019). Antibacterial properties of
648 nanofibers containing chrysanthemum essential oil and their application as beef
649 packaging. *International Journal of Food Microbiology*, *292*(December 2018), 21–
650 30. https://doi.org/10.1016/j.ijfoodmicro.2018.12.007
651 Mansur, H. S., Sadahira, C. M., Souza, A. N., & Mansur, A. A. P. (2008). FTIR
652 spectroscopy characterization of poly (vinyl alcohol) hydrogel with different
653 hydrolysis degree and chemically crosslinked with glutaraldehyde. *Materials*
654 *Science and Engineering C*, *28*(4), 539–548.
655 https://doi.org/10.1016/j.msec.2007.10.088
656 Miraftab, M., Saifullah, A. N., & Çay, A. (2015). Physical stabilisation of electrospun
657 poly(vinyl alcohol) nanofibres: comparative study on methanol and heat-based
658 crosslinking. *Journal of Materials Science*, *50*(4), 1943–1957.
659 https://doi.org/10.1007/s10853-014-8759-1
660 Neo, Y. P., Swift, S., Ray, S., Gizdavic-Nikolaidis, M., Jin, J., & Perera, C. O. (2013).
661 Evaluation of gallic acid loaded zein sub-micron electrospun fibre mats as novel
662 active packaging materials. *Food Chemistry*, *141*(3), 3192–3200.
663 https://doi.org/10.1016/j.foodchem.2013.06.018
664 Nikfarjam, N., Taheri Qazvini, N., & Deng, Y. (2014). Cross-linked starch
665 nanoparticles stabilized Pickering emulsion polymerization of styrene in w/o/w
666 system. *Colloid and Polymer Science*, *292*(3), 599–612.
667 https://doi.org/10.1007/s00396-013-3102-y
668 Ntzimani, A. G., Paleologos, E. K., Savvaidis, I. N., & Kontominas, M. G. (2008).
669 Formation of biogenic amines and relation to microbial flora and sensory changes
670 in smoked turkey breast fillets stored under various packaging conditions at 4 °C.

Food Microbiology, *25*(3), 509–517. https://doi.org/10.1016/j.fm.2007.12.002

Ojeda-sana, A. M., Baren, C. M. Van, Elechosa, M. A., Juárez, M. A., & Moreno, S. (2013). New insights into antibacterial and antioxidant activities of rosemary essential oils and their main components. *Food Control*, *31*(1), 189–195. https://doi.org/10.1016/j.foodcont.2012.09.022

Peresin, M. S., Vesterinen, A. H., Habibi, Y., Johansson, L. S., Pawlak, J. J., Nevzorov, A. A., & Rojas, O. J. (2014). Crosslinked PVOH nanofibers reinforced with cellulose nanocrystals: Water interactions and thermomechanical properties. *Journal of Applied Polymer Science*, *131*(11), 1–12. https://doi.org/10.1002/app.40334

Pinheiro Bruni, G., de Oliveira, J. P., Gómez-Mascaraque, L. G., Fabra, M. J., Guimarães Martins, V., Zavareze, E. da R., & López-Rubio, A. (2020). Electrospun β-carotene–loaded SPI:PVOH fiber mats produced by emulsion-electrospinning as bioactive coatings for food packaging. *Food Packaging and Shelf Life*, *23*(October 2019), 100426. https://doi.org/10.1016/j.fpsl.2019.100426

Ramos, C., Teixeira, B., Batista, I., Matos, O., Serrano, C., Neng, N. R., … Marques, A. (2012). Antioxidant and antibacterial activity of essential oil and extracts of bay laurel Laurus nobilis Linnaeus (Lauraceae) from Portugal Antioxidant and antibacterial activity of essential oil and extracts of bay laurel Laurus nobilis Linnaeus (Lauraceae) fro. *Natural Product Research*, *26*(6), 518–529. https://doi.org/10.1080/14786419.2010.531478

Ramos, M., Jiménez, A., Peltzer, M., & Garrigós, M. C. (2012). Characterization and antimicrobial activity studies of polypropylene films with carvacrol and thymol for active packaging. *Journal of Food Engineering*, *109*(3), 513–519. https://doi.org/10.1016/j.jfoodeng.2011.10.031

696 Sánchez-González, L., Vargas, M., González-Martínez, C., Chiralt, A., & Cháfer, M.
697 (2011). Use of Essential Oils in Bioactive Edible Coatings: A Review. *Food*
698 *Engineering Reviews*, *3*(1), 1–16. https://doi.org/10.1007/s12393-010-9031-3
699 Santiago-Morales, J., Amariei, G., Letón, P., & Rosal, R. (2016). Antimicrobial activity
700 of poly(vinyl alcohol)-poly(acrylic acid) electrospun nanofibers. *Colloids and*
701 *Surfaces B: Biointerfaces*, *146*, 144–151.
702 https://doi.org/10.1016/j.colsurfb.2016.04.052
703 Shi, R., Bi, J., Zhang, Z., Zhu, A., Chen, D., Zhou, X., … Tian, W. (2008). The effect of
704 citric acid on the structural properties and cytotoxicity of the polyvinyl
705 alcohol/starch films when molding at high temperature. *Carbohydrate Polymers*,
706 *74*(4), 763–770. https://doi.org/10.1016/J.CARBPOL.2008.04.045
707 Stone, S. A., Gosavi, P., Athauda, T. J., & Ozer, R. R. (2013). In situ citric acid
708 crosslinking of alginate/polyvinyl alcohol electrospun nanofibers. *Materials*
709 *Letters*, *112*, 32–35. https://doi.org/10.1016/J.MATLET.2013.08.100
710 Suganthi, S., Mohanapriya, S., Raj, V., Kanaga, S., Dhandapani, R., Vignesh, S., &
711 Kalyana Sundar, J. (2018). Tunable Physicochemical and Bactericidal Activity of
712 Multicarboxylic-Acids-Crosslinked Polyvinyl Alcohol Membrane for Food
713 Packaging Applications. *ChemistrySelect*, *3*(40), 11167–11176.
714 https://doi.org/10.1002/slct.201801851
715 Tian, H., Yan, J., Rajulu, A. V., Xiang, A., & Luo, X. (2017). Fabrication and properties
716 of polyvinyl alcohol/starch blend films: Effect of composition and humidity.
717 *International Journal of Biological Macromolecules*, *96*, 518–523.
718 https://doi.org/10.1016/j.ijbiomac.2016.12.067
719 Van Etten, E. A., Ximenes, E. S., Tarasconi, L. T., Garcia, I. T. S., Forte, M. M. C., &
720 Boudinov, H. (2014). Insulating characteristics of polyvinyl alcohol for integrated

721 electronics. *Thin Solid Films*, *568*(1), 111–116.
722 https://doi.org/10.1016/j.tsf.2014.07.051
723 Vinci, G., & Antonelli, M. L. (2002). Biogenic amines: Quality index of freshness in
724 red and white meat. *Food Control*, *13*(8), 519–524. https://doi.org/10.1016/S0956-
725 7135(02)00031-2
726 Wyrzykowski, D., Hebanowska, E., Nowak-Wiczk, G., Makowski, M., &
727 Chmurzyński, L. (2011). Thermal behaviour of citric acid and isomeric aconitic
728 acids. *Journal of Thermal Analysis and Calorimetry*, *104*(2), 731–735.
729 https://doi.org/10.1007/s10973-010-1015-2
730 Yang, D., Li, Y., & Nie, J. (2007). Preparation of gelatin/PVOH nanofibers and their
731 potential application in controlled release of drugs. *Carbohydrate Polymers*, *69*(3),
732 538–543. https://doi.org/10.1016/j.carbpol.2007.01.008
733 Yen, H. F., Hsieh, C. T., Hsieh, T. J., Chang, F. R., & Wang, C. K. (2015). In vitro anti-
734 diabetic effect and chemical component analysis of 29 essential oils products.
735 *Journal of Food and Drug Analysis*, *23*(1), 124–129.
736 https://doi.org/10.1016/j.jfda.2014.02.004
737 Zhang, Y., Zhang, Y., Zhu, Z., Jiao, X., Shang, Y., & Wen, Y. (2019). Encapsulation of
738 thymol in biodegradable nanofiber via coaxial eletrospinning and applications in
739 fruit preservation. *Journal of Agricultural and Food Chemistry*, *67*(6), 1736–1741.
740 https://doi.org/10.1021/acs.jafc.8b06362
741
742
743